Soft Matter

Accepted Manuscript

ROYAL SOCIETY OF CHEMISTRY

www.rsc.org/softmatter

Coarse Grain Forces in Star Polymer Melts

L. Liu, W.K. den Otter, and W.J. Briels*

Computational Biophysics, MESA+, University of Twente,

P.O. Box 217, 7500 AE, Enschede, The Netherlands

(Dated: July 16, 2014)

Abstract

An analysis is presented of forces acting on the centers of mass of three-armed star polymers in the molten state. The arms consist of 35 Kremer-Grest beads, which is slightly larger than needed for one entanglement mass. For a given configuration of the centers of mass, instantaneous forces fluctuate wildly around averages which are two orders of magnitude smaller than their root mean square deviations. Average forces are well described by an implicit many-body potential, while pair models fail completely. The fluctuating forces are modelled by means of dynamical variables quantifying the degree of mixing of the various polymer pairs. All functions and parameters in a coarse grain model based on these concepts are obtained from the underlying small scale simulation. The coarse model reproduces both the diffusion coefficient and the shear relaxation modulus. Ways to improve the model suggest themselves on the basis of our findings.

* w.j.briels@utwente.nl

I. INTRODUCTION

Polymer melts and solutions exhibit dynamics on a wide range of time and length scales. The individual atoms move at time scales of picoseconds while groups of atoms move on time scales of nanoseconds. In an entangled system whole chains can move only by reptation [1, 2] while branched polymers move by arm retraction followed by displacements of the branch points[3]. Time scales corresponding to these processes are microseconds or longer. Different experimental techniques are needed to investigate different length and time scales. Neutron spin echo techniques may be used to study time scales up to a few hundred nanoseconds, while mechanical spectroscopy typically probes time scales larger than miliseconds.

Also computational studies of polymer systems require different models to investigate different time and length scales. This is not only due to computational limitations, but also results from the physicists wish to develop concepts and understanding on the basis of minimalistic models[4, 5]. If one wants to understand chemical aspects, clearly atomistic[6] or slightly coarse grained[7] models are needed. On the other hand, if one wants to understand long time motions of polymer chains, what matters are chain connectivity and uncrossability. The minimalistic model in this case is the famous Kremer-Grest model[8], which has been used to understand how and why properties change with changing lengths of the chains. Several other models have been developed to handle even longer time scales by resorting to even coarser descriptions[9–14].

In recent years, we developed a model that intends to go even one step further than the models described above. Where the models described above are used to investigate material properties, we intend to devise a model that is capable of describing flow of polymer systems, or soft matter in general, in complicated geometries. This is the realm where usually computational fluid dynamics (CFD) methods are used based on one out of many constitutive models[15, 16] governing the relation between stresses and velocity gradients. Such models, however, are applicable only in their own limited ranges of experimental conditions. For example in polymer solutions, one may expect strong correlations between concentrations and velocity gradients[17, 18]. Such couplings and the instabilities they give rise to are absent in the usual constitutive models, with only very few exceptions.

In order to allow for simulations of very large systems, the model that we developed is necessarily very coarse. Each polymer is represented by one single point particle[19].

Obviously these particles must be dressed with additional properties in order to take into account the response of all eliminated degrees of freedom to the ever changing circumstances provided by the configurations of the polymer positions and their histories[20]. This is reflected in the name of the model, i.e. responsive particle dynamics (RaPiD). The model is developed such that it automatically conserves the exact thermodynamic properties of the underlying real system. Moreover, by being a particle based simulation model, it automatically allows for concentration gradients and fluctuations necessary to initiate possible flow instabilities[21, 22].

Until now we have applied the model by tuning its various parameters to experimental data[23–28]. In order to further test the model and investigate its conceptual soundness we want to directly calculate its various functions and parameters from data generated by a small scale simulation. The degree to which this is possible and the quality of its predictions are the subject of this paper. In section II we describe the model and the ratio behind its particular structure. In section III we describe how we intend to calculate the RaPiD functions and parameters from the data obtained with a small scale simulation. The small scale system in this case is a three arm star polymer melt built from Kremer-Grest polymers under melt conditions. In section IV we shortly describe this model and its simulation. In section V we present our results of mapping the small scale simulation results on our coarse RaPiD model. Finally we present a summary and some conclusions in section VI.

Before diving into the subject of this paper, let us briefly describe the concepts and context of the RaPiD model. Besides being a model to perform mesoscopic simulations, the model provides tools to discuss mesoscopic processes in flowing soft matter. Several unknown functions and parameters describing these processes are introduced on a phenomenological basis. These model functions must be related to more fundamental processes at the atomistic or slightly coarse grain level. From this point of view one might consider the model to be a constitutive model at the mesoscopic level. The model assumes that coarse entities may be identified that suffice to discuss the flow. For example, with polymer solutions one typically notices that complete macromolecules are displacecd by the flow, so it is natural to consider macromolecules devoid of internal structure. One should not expect, however, that these structureless macromolecules move like large atoms experiencing conservative forces determined by their positions alone. Besides the usual friction (and corresponding random) forces, RaPiD makes use of transient forces that take into account the coupling between

internal and external degrees of freedom when the particles are displaced with respect to each other. For enlightening pictures showing this coupling see Ref[21] and Ref[29].

II. COARSE GRAINING

In this section we collect some pertinent information about coarse graining. In order not to make the discussion unnecessary complicated by presenting the most general equations, we illustrate the coarse graining procedure by applying it to a melt of star polymer.

We consider a melt of N star polymers in a volume V. Each polymer consists of a central bead, also called branch point, to which f arms of m beads each are connected. The mass of the polymer is $M = mf + 1$. At the coarse level we want to describe the configuration of the melt by a set of N position vectors $\vec{R}_n$, while all other degrees of freedom will be eliminated from the description. The elimination should be done such that as many properties as possible of the original system are described correctly by the coarse model. In particular, we would like to retain the correct dynamics and the correct thermodynamics of the system. Obviously, properties which are defined in terms of the eliminated degrees of freedom cannot be calculated from the trajectories of the coarse model.

There are two natural choices for $\vec{R}_n$, either the position of the branch point of star n, or the position of its center of mass. In this paper we adopt the second definition, i.e. $\vec{R}_n$ denotes the center of mass position vector of the n'th star. The reason for this is that with this choice $\vec{R}_n$ doesn't accelerate in case the total force acting on the star is zero. A second reason for this choice is that the motion of the centers of mass is much smoother than that of the branch points.

Let us first consider the Hamiltonian of our system. Denoting $\vec{x}_{ni}$ the position vector of the beads, with n numbering from 1 to N and i from 0 to mf and $\vec{x}_{n0}$ being the position vector of the central bead of the n'th star, we define

$$\vec{R}_n = \frac{1}{M}\sum_{i=0}^{mf} \vec{x}_{ni}. \tag{1}$$

$$\vec{q}_{ni} = \vec{x}_{ni} - \vec{R}_n, \quad i = 1, ..., mf. \tag{2}$$

The Hamiltonian may then readily be shown to be

$$H = \frac{1}{2M}\sum_{n=1}^{N} \vec{P}_n^2 + \frac{1}{2}\sum_{n=1}^{N}\sum_{i=1}^{mf} \vec{p}_{ni}^{\,2} - \frac{1}{2M}\sum_{n=1}^{N}(\sum_{i=1}^{mf} \vec{p}_{ni})^2 + V(R, q). \tag{3}$$

with

$$\vec{P}_n = M\dot{\vec{R}}_n. \tag{4}$$

$$\vec{p}_{ni} = \dot{\vec{q}}_{ni} + \sum_{j=1}^{mf} \dot{\vec{q}}_{nj}. \tag{5}$$

R denotes the set of all vectors $\vec{R}_n$ and q the set of all vectors $\vec{q}_{ni}$; a dot over a symbol denotes a time derivative and $V(R,q)$ is the potential energy of the configuration (R,q).

Since the kinetic energy does not depend on (R,q), we have

$$\dot{\vec{P}}_n = -\frac{\partial H}{\partial \vec{R}_n} = -\frac{\partial V}{\partial \vec{R}_n}. \tag{6}$$

The general strategy of coarse graining is to manipulate the force in the right hand side such that the contributions of all $\vec{p}_{ni}$ and $\vec{q}_{ni}$ are lumped into a few functions that can easily be modeled. The first step is to separate the average force[30], so

$$-\frac{\partial V}{\partial \vec{R}_n} = -\left\langle \frac{\partial V}{\partial \vec{R}_n} \right\rangle_B + \vec{G}_n. \tag{7}$$

The pointy brackets $\langle \cdots \rangle_B$ denote an average over all $\vec{p}_{ni}$ and $\vec{q}_{ni}$; $\vec{G}_n$ is what remains of the force.

In the next two sections we will describe the two contributions to the force.

A. Potential of mean force

The average force introduced in Eq. (7) is defined as

$$-\left\langle \frac{\partial V}{\partial \vec{R}_n} \right\rangle_B = -\frac{1}{Q} \int dq \int dp e^{-\beta H} \frac{\partial V}{\partial \vec{R}_n}. \tag{8}$$

where $\int dq$ indicates an integral over all $\vec{q}_{ni}$ and $\int dp$ an integral over all $\vec{p}_{ni}$; moreover $Q = \int dq \int dp e^{-\beta H}$. Since the kinetic energy in Eq. (3) does not depend on any of q_{ni}, the integrals over p lead to constant factors which cancel in the numerator and the denominator, so

$$-\left\langle \frac{\partial V}{\partial \vec{R}_n} \right\rangle_B = -\frac{\partial \Phi}{\partial \vec{R}_n}. \tag{9}$$

where

$$\Phi(R) = -k_B T \ln \int dq e^{-\beta V(R,q)}. \tag{10}$$

We call Φ the potential of mean force. Apart from some uninteresting constants, it is equal to the free energy of the $\vec{q}_{ni}$ in a field produced by the interactions with the fixed $\vec{R}_n$.

Once we have completed our manipulations of $\vec{G}_n$ in the next section, we will find that a simulation of the coarse system samples the probability distribution

$$P(R) \sim \exp\{-\beta\Phi(R)\}. \tag{11}$$

This implies that all thermodynamic properties obtained from simulations of the coarse model derive from the free energy

$$A = -k_B T \ln \int dR e^{-\beta\Phi(R)}. \tag{12}$$

Introducing the definition of $\Phi(R)$ we obtain

$$A = -k_B T \ln \int dR \int dq e^{-\beta V(R,q)}. \tag{13}$$

Apart from some constants resulting from integrals over all momenta and from a factor $(h^{3N}N!)^{-1}$ in the partition function, A is the exact free energy of the microscopic system[31].

Whether or not we are able to obtain the exact thermodynamics from a coarse model depends on our ability to find a functional form describing $\Phi(R)$ for all configurations that contribute to the integral in Eq. (12), i.e. whether we are able to faithfully represent $\Phi(R)$. The usual approach is to assume that $\Phi(R)$ may be approximated as a sum of contributions from each pair of polymers

$$\Phi(R) = \sum_{i=1}^{N-1} \sum_{j=i+1}^{N} \phi(R_{ij}). \tag{14}$$

Besides applying the pair approximation we have assumed that each contribution depends only on the distance between the two polymers that constitute the pairs. In the case of star polymers, explicit expressions for $\phi(R_{ij})$ have been presented by Löwen, Likos and co-workers[32, 33]. For our case, i.e. stars with a functionality of three, they write:

$$\begin{aligned} \phi(r) &= -\frac{5}{8} k_B T f^{3/2} [\ln(\frac{r}{\sigma_s}) - \frac{1}{2\tau^2\sigma_s^2}], && r \le \sigma_s \\ &= -\frac{5}{8} k_B T f^{3/2} \frac{1}{2\tau^2\sigma_s^2} \exp\{-\tau^2(r^2 - \sigma_s^2)\}, && r > \sigma_s. \end{aligned} \tag{15}$$

Here $\tau\sigma_s = 1.06$ and $\sigma_s = \frac{4}{3}R_g$, with R_g the radius of gyration of the star. In our case $f = 3$.

It is clear that with a functionality as low as three, when the arms are very long, each polymer will interact with many other polymers, not just with its first neighbours. In this

situation we may expect many-body interactions to be important. It is well known that it is very difficult to collect information about many-body contributions to the potential energy, free energy in our case, and to develop some intuitive understanding. Therefore, stimulated by the literature on density functional methods[34] and the work of Pagonabarraga and Frenkel[35], in recent years we have made extensive use[23, 24, 28] of an implicit many-body potential in which $\Phi(R)$ is written as

$$\Phi_{\rm FH}(R) = \sum_i a(\eta_i(R)). \tag{16}$$

Here $\eta_i(R)$ is the local volume fraction of polymers at the position $\vec{R}_i$ defined below; $a(\eta)$ is the free energy of one polymer in a melt of volume fraction η. The contribution of the translational configurations of the centers of mass must be excluded from $\Phi_{\rm FH}(R)$. When calculating the Flory-Huggins free energy $\Phi_{\rm FH}(R)$ we treat the star polymer as being equivalent to a linear polymer consisting of p Kuhn lengths, obtaining

$$a(\eta) = k_B T p\{\frac{1-\eta}{\eta} ln(1-\eta) - \chi\eta\}. \tag{17}$$

The Flory-Huggins parameter χ accounts for minus the interaction energy between two Kuhn lengths.

The local volume fraction of polymers is defined as

$$\eta_i(R) = \frac{1}{\rho_{max}} \sum_{j\neq i} w(R_{ij}). \tag{18}$$

where $w(R_{ij})$ is a normalized weight function, i.e. $\int d^3R w(R) = 1$, implying that for a random distribution of polymers $\sum_j w(R_{ij}) = N/V = \bar{\rho}$. It has been argued by Trofimov *et al.*[36] that the sum in Eq. (14) should exclude the term when $j = i$.

Because of crowding near the branch point we expect that each polymer excludes the others from approaching very closely. We therefore add short-range repulsive pair potentials to the Flory-Huggins potential obtaining

$$\Phi(R) = \Phi_{\rm FH}(R) + \sum_{i=1}^{N-1} \sum_{j=i+1}^{N} \phi^{rep}(R_{ij}). \tag{19}$$

Notice that here it might have been better to let R_{ij} be the distance between two branch points instead of the distance between two centers of mass.

B. Transient forces

The thermodynamic forces described in the previous section provide a reasonable estimate of the exact instantaneous forces only in case the dynamics of the eliminated degrees of freedom is much faster than that of the retained degree of freedom. As an example one may think of hard sphere colloids dissolved in a solution of small polymers which move much faster than the colloids. The forces exerted by the polymers on the colloids are well represented by depletion forces between the colloids. The remaining forces defined in Eq. (7) are then simple friction forces and corresponding random forces.

The situation is completely different in cases when the eliminated degrees of freedom are not much faster than the retained degrees of freedom, for example when the relaxation of the arms of a star polymer towards equilibrium is not much faster than the time scales during which the centers of mass of the polymers diffuse over length scales comparable to their sizes. In these cases, knowledge of the positions (and momenta) of the centers of mass of the stars gives little or no information on the state of the eliminated degrees of freedom. The system can arrive at one and the same coarse state (R, P) in many different ways distinguished by many different states (q, p) of the arms and different instantaneous forces on the centers of mass. The only way to obtain some information about the state of the arms by interrogating the configurations of the centers of mass, is to keep track of its full history. This is why the Mori-Zwanzig projection[37, 38] operator formalism leads to very complicated friction forces with memory and corresponding random forces. One way to model these friction forces is to define additional variables which give a rough description of the states of the arms and to provide a propagator which describes its dynamics. This is what we will do next.

We assume[20] that with every configuration R of the centers of mass we may associate a thermodynamic equilibrium state of the arms, and that this state may be characterized by a collection of numbers $\{n_0(R_{ij}) \mid R_{ij} \leq R_c\}$. The free energy of this state is equal to the potential of mean force discussed in the previous section. We next introduce a collection of dynamical variables $\{n_{ij} \mid R_{ij} \leq R_c\}$ and let the deviations of these numbers from the corresponding equilibrium numbers, i.e. $\{n_{ij} - n_0(R_{ij}) \mid R_{ij} \leq R_c\}$, describe the deviation from equilibrium. We call n_{ij} the contact numbers between stars i and j, and $n_0(R_{ij})$ the corresponding equilibrium contact number. Other names, like mixing number or entanglement number, have also been used. The contact numbers must be thought of

as thermodynamic variables like the variables used in Landau-de Gennes types of theories. Finally, we assume that the free energy for a given configuration R of the centers of mass and with the contact numbers constrained to the values $n = \{n_{ij}\}$ is given by

$$A(R,n) = \Phi(R) + \frac{1}{2}\alpha \sum_{i=1}^{N-1} \sum_{j=i+1}^{N} \{n_{ij} - n_0(R_{ij})\}^2, \tag{20}$$

where n_{ij} and $n_0(R_{ij})$ are non-existent when $R_{ij} > R_c$. The force on polymer i is now

$$\begin{aligned} \vec{F}_i &= -\frac{\partial A}{\partial \vec{R}_i} + \vec{G}_i' \\ &= -\frac{\partial \Phi}{\partial \vec{R}_i} + \alpha \sum_j \{n_{ij} - n_0(R_{ij})\} \frac{dn_0}{dR_{ij}} \frac{\vec{R}_{ij}}{R_{ij}} + \vec{G}_i' \end{aligned} \tag{21}$$

Notice that $\vec{G}_i'$ is different from $\vec{G}_i$ in Eq. (7). The second term in Eq. (21) is called the transient force $\vec{F}_i^t$ for reasons explained in the next section. Notice that α may be called the strength of the transient forces.

In the next section we will present a propagator which samples from the distribution

$$P(R,n) \sim \exp\{-\beta A(R,n)\}. \tag{22}$$

Suppose we are only interested in the distribution of the centers of mass, i.e. we integrate $P(R,n)$ over all values of n, we obtain

$$P(R) = \int dn P(R,n) \sim \exp\{-\beta \Phi(R)\}. \tag{23}$$

This means that all structural and thermodynamic properties of the system are the same as before the introduction of the transient forces.

We now turn to the propagator.

III. BROWNIAN DYNAMICS

We assume that with the introduction of the transient forces all memory effects are taken into account. The remaining forces $\vec{G}_i'$ on polymer i are then simple friction forces and corresponding Markovian random forces. Markovian means that the random forces are δ-correlated in time.

Since soft matter systems are usually overdamped, we ignore momenta and make use of a simple first order propagator. For simple Markovian systems Ermak and McCammon[39]

have shown how to derive the Brownian propagator from a second order Langevin equation. Here we simply pose the result

$$d\vec{R}_i = -\frac{1}{\xi_i}\frac{\partial A}{\partial \vec{R}_i}dt + \frac{\partial}{\partial \vec{R}_i}\frac{k_B T}{\xi_i}dt + \sqrt{\frac{2k_B T dt}{\xi_i}}\vec{\Theta}_i. \tag{24}$$

Here $d\vec{R}_i$ is the displacement of particle i during a time-interval from t to $t+dt$. On the right-hand side ξ_i is the friction coefficient of particle i, which depends on the configuration at time t, and $\vec{\Theta}_i$ is a random vector associated with particle i at time t. $\vec{\Theta}_i$ is independent of random vectors associated with other particles and independent of random vectors at other times than time t; moreover the components of $\vec{\Theta}_i$ are uncorrelated and have zero mean and unit variance. The second term in the right hand side of Eq. (24) is needed to ensure, together with the propagator for the contact numbers, the correct equilibrium distribution Eq. (22).

In principle, we have some freedom in choosing the propagator for the contact numbers. However, if we want to have the equilibrium distribution as the stationary solution, we are forced to use[20]

$$dn_{ij} = -\frac{1}{\tilde{\xi}}\frac{\partial A}{\partial n_{ij}}dt + \sqrt{\frac{2k_B T dt}{\tilde{\xi}}}\Theta_{ij}. \tag{25}$$

Here dn_{ij} is the increment of n_{ij} during a time interval of length dt. $\tilde{\xi}$ is a friction similar to the one in the propagator for $\vec{R}_i$. It is taken to be independent of the n_{ij}. In previous applications it was sometimes assumed to depend on R_{ij}, but in this paper it will be constant. Finally Θ_{ij} is a random number associated with the pair ij at time t, uncorrelated from any other random numbers and having zero mean and unit variance.

In the following we will replace $\tilde{\xi}$ by $\alpha\mu$, where μ has the dimension of time. Performing the differentiation in Eq. (25) we obtain

$$dn_{ij} = -\frac{n_{ij} - n_0(R_{ij})}{\mu}dt + \sqrt{\frac{2k_B T dt}{\alpha\mu}}\Theta_{ij}. \tag{26}$$

i.e. a simple kinetic equation with a random contribution. If we consider the contact variables as thermodynamic variables, then Eq. (26) resembles the evolution equation used in irreversible thermodynamics[40] with $1/\mu$ being the Onsager coefficient.

Suppose we fix the centers of mass $\vec{R}_i$, then the contact numbers will gradually decay towards their equilibrium values and finally fluctuate around the latter. This is why the $\vec{F}_i^t$

are called transient forces. The physical picture is that always the contact numbers decay towards their equilibrium values, but that the latter continually change due to displacements of the particles.

Since our model consists of structureless particles, there are only two timescales in our model. One is set by the thermodynamic forces, derived from the potential of mean force, and the friction coefficient ξ_0 in Eq. (35). The other is similarly set by the strength of the transient forces and the corresponding friction $\tilde{\xi}$, i.e. by $\mu = \tilde{\xi}/\alpha$. The rheology of the model will therefore closely resemble a two-time Maxwell model. If one wants to introduce a continuous range of characteristic times, this may be done by making μ dependent on the distance between the contacting polymers, for example according to[41]

$$\mu(R_{ij}) = \mu e^{-R_{ij}/\lambda}. \tag{27}$$

In the present application we will restrict ourselves to constant $\mu(R_{ij}) = \mu$, i.e. to $\lambda = \infty$. We leave a more realistic description for future investigations.

In case we want to calculate the parameters and functions in our coarse model, we must choose a mechanical interpretation of the contact numbers, in particular we must present a mechanical definition of n_{ij}. This we will do in the next section.

IV. COARSE PARAMETERS FROM SMALL SCALE SIMULATIONS

In this section we describe our choices for the functions introduced in the previous section and how they will be obtained from a small scale simulation.

We start with the description of functions and parameters appearing in the Flory-Huggins free-energy. In this work we adopt the weight function introduced by Santos de Oliveira *et al.*[23]:

$$\begin{aligned} w(R_{ij}) &= C(R_c - R_s)(R_c + R_s - 2R_{ij}), && R_{ij} \leq R_s \\ &= C(R_{ij} - R_c)^2, && R_s < R_{ij} \leq R_c \\ &= 0 && R_c < R_{ij}. \end{aligned} \tag{28}$$

Here C takes care of the normalizations. R_c and R_s are two adjustable parameters. In earlier work by Kindt and Briels it was found that a linear weight function performs best; the second, quadratic regime has been included to smoothen the function at $R_{ij} = R_c$. Since

each polymer has no direct knowledge of things happening at a distance larger than a few times its radius of gyration R_g, we expect that $R_c \simeq 2.5R_g$; around this value R_c and R_s may be used as adjustable parameters. Besides these, there are three more parameters, i.e. ρ_{max}, p and χ, that will be treated as adjustable parameters. All three of them may be roughly estimated on the basis of their physical meaning. The range within which these parameters can be varied is therefore very small.

Next we consider the transient forces. Our intuitive picture of equilibrium between two nearby star polymers is that their arms are mixed such that there is a well defined number of contacts between the beads from one polymer with those from the other polymer. In general the number of contacts between two stars in equilibrium with each other will decrease with the distance between the stars. If we quickly bring two stars in equilibrium closer together, it will take some time for the stars to adjust to the new situation and to increase their mutual contacts. During this time the stars are out of equilibrium. Similarly on increasing the distance between two stars it takes some time before the stars have decreased their mutual contact number. Again, during this period the stars are out of equilibrium. From this picture it emerges that a decent definition for n_{ij} might be

$$n_{ij} = C \sum_k \sum_l X_\Delta(\mid \vec{x}_{ik} - \vec{x}_{jl} \mid). \tag{29}$$

with

$$\begin{aligned} X_\Delta(r) &= 1, \quad r \leq \Delta \\ &= 0, \quad r > \Delta \end{aligned} \tag{30}$$

This indeed is the definition that we adopt. The constant C will be defined below. Other definitions may be conceivable depending on the application. In particular it would be useful for linear polymers to define n_{ij} such that it captures the number of topological constraints between polymers i and j.

Given a working definition to calculate n_{ij}, we may calculate $n_0(R_{ij})$ from an equilibrium simulation of the small scale system. To this end, for each frame of the small scale equilibrium run, we run through all pairs, calculate their n_{ij} and R_{ij} , and put n_{ij} in the bin corresponding to R_{ij}. Finally we average the values of n_{ij} in each bin independently. In this paper we will normalize $n_0(R_{ij})$ such that $n_0(0) = 1$; this fixes the constant C in Eq. (29). The reader must be aware that different normalizations lead to different values of α. With this

normalization, we will find that $n(R_{ij})$ is rather insensitive for the precise value of Δ in Eq. (29).

In a similar way we calculate the variance $\langle (n_{ij} - n_0(R_{ij}))^2 \rangle$ for every bin, and next calculate α from the equipartition theorem

$$\langle (n_{ij} - n_0(R_{ij}))^2 \rangle = \frac{k_B T}{\alpha(R_{ij})}. \tag{31}$$

which may be obtained with the use of Eq. (16). Notice that here we assume that α may depend on R_{ij}. This will actually turn out to be true. Since our intention is to only give a proof of principle of the methods presented in this paper we will ignore this fact and take α to be constant.

Finally we must calculate ξ_i and μ. As already mentioned, in a simulation with fixed centers of mass the contact numbers n_{ij} will initially decay towards their equilibrium values and then fluctuate around them. This allows for two possible ways to calculate μ. First, we may keep track of the individual time evolutions $\Delta n_{ij}(t) = n_{ij}(t) - n_0(R_{ij})$ right after the centers of mass have been fixed, and average these curves for all pairs (i, j), after dividing by $\Delta n_{ij}(0)$. According to Eq. (26) the result will be $e^{-t/\mu}$. Because not all of the sampled functions are equally relevant from a statistical point of view, we introduce a weight w_{ij} with every pair (i, j) when we average over pairs, so

$$\sum_{\langle i,j \rangle} \frac{\Delta n_{ij}(t)}{\Delta n_{ij}(0)} w_{ij} = e^{-t/\mu}. \tag{32}$$

It is clear that pairs for which the absolute value of $\Delta n_{ij}(0)$ is large should have a larger weight than those for which the absolute value of $\Delta n_{ij}(0)$ is small. Therefore we adopt a weight w_{ij} proportional to $\Delta n_{ij}(0)^2$. This then leads to

$$\frac{\frac{1}{N_p} \sum_{\langle i,j \rangle} \Delta n_{ij}(t) \Delta n_{ij}(0)}{\frac{1}{N_p} \sum_{\langle i,j \rangle} \Delta n_{ij}(0)^2} = e^{-t/\mu}. \tag{33}$$

Here N_p is the number of pairs occurring in the sum over pairs. A second approach might be based on Onsager's regression hypothesis[42, 43], which says that equilibrium fluctuations on average decay according to the corresponding macroscopic laws. As a result

$$\frac{\langle \Delta n_{ij}(t) \Delta n_{ij}(0) \rangle}{\langle \Delta n_{ij}(0)^2 \rangle} = e^{-t/\mu}. \tag{34}$$

Here, $\langle \cdots \rangle$ indicates an average over initial times followed by an average over pairs. Notice the similarity between both methods. Here we adopt the first method since it is computationally less demanding.

The last remaining quantity that we must specify is the friction ξ_i. Here ξ_i is assumed to depend on the instantaneous configuration through[23]

$$\xi_i = \xi_0 \sum_{j \neq i} \sqrt{\mid n_{ij} \mid n_0(R_{ij})}, \tag{35}$$

i.e. roughly proportional to the instantaneous contact number n_{ij}. The specific choice with the square root of $\mid n_{ij} \mid n_0(R_{ij})$ is made to have the function equal to zero for values of R_{ij} larger than R_c. The constant ξ_0 may be interpreted as the friction per contact. Although in principle it is possible to measure this parameter from a small scale simulation, see Padding and Briels[12], this is statistically very demanding and we will not do so. Instead we will adjust ξ_0 in order to have the diffusion coefficient of the coarse model equal to that of the small scale model.

Once all parameters have been calculated according to the methods presented in this section, the rheology of the coarse method should be equal to that of the small scale model. Of course we should not expect that the microscopic shear relaxation modulus $G(t)$ be reproduced by the coarse model in all details, but the absolute values and time scales should be roughly in agreement. For better agreement on all time scales, the coarse model should be enriched with more detail, as for example in Eq. (27).

V. SET UP OF SMALL SCALE SIMULATIONS

For the small scale molecular dynamics (MD) model of our star polymer melt, we have selected the widely applied Kremer-Grest polymer model [8]. In brief, any pair of particles separated by a distance r interacts by a Weeks-Chandler-Andersen (WCA) potential,

$$U(r) = \begin{cases} 4\epsilon \left[\left(\frac{\sigma}{r}\right)^{12} - \left(\frac{\sigma}{r}\right)^{6} + \frac{1}{4} \right] & , \quad r < 2^{1/6}\sigma \\ 0 & , \quad r \geq 2^{1/6}\sigma, \end{cases} \tag{36}$$

with interaction strength ϵ and diameter σ. Bonds between adjacent beads in a chain are modelled by a finitely extensible nonlinear elastic (FENE) potential,

$$U(r) = \begin{cases} -\frac{1}{2} k R_0^2 \ln \left[1 - (\frac{r}{R_0})^2 \right] & , \quad r < R_0 \\ \infty & , \quad r \geq R_0, \end{cases} \tag{37}$$

with spring constant $k = 30\epsilon/\sigma^2$ and maximum bond length $R_0 = 1.5\sigma$. All particles have the same mass m.

The MD simulations of this small scale model were run in Gromacs 4.6 [44], using the leap-frog stochastic dynamics integrator. This algorithm discretizes the Langevin equation of motion for particle i,

$$m\ddot{\vec{x}}_i = -\vec{\nabla}_i U - \gamma m\dot{\vec{x}}_i + \vec{f}_i(t), \tag{38}$$

with total potential energy U, friction coefficient γ and a Markovian random force $\vec{f}_i$ sampled from a Gaussian distribution. The friction and random forces collectively act as a thermostat, by the fluctuation-dissipation theorem, maintaining a temperature T. We follow the choices made by Kremer and Grest in presenting numerical values by reduced units where $\sigma = \epsilon = m = 1$ and $k_B T = \epsilon$, a bead density of $0.85\sigma^{-3}$ and $\gamma = 0.5\tau^{-1}$, with time unit $\tau = \sigma\sqrt{m/\epsilon}$. The simulation time step was set at $1 \times 10^{-3}\tau$. Static and dynamic properties of linear and star polymers simulated with this small scale model are extensively discussed in Refs [8] and [45].

The simulation box contained 300 star polymers, each consisting of three arms of 35 beads – corresponding to approximately one entanglement length – connected to a central bead. The 31,800 beads were confined in a cubic simulation box with periodic boundary conditions. Starting boxes were created by growing randomly generated chains at random positions in the box; each additional bead was placed randomly in a spherical shell centered around its previously inserted covalent neighbour, whilst rejecting any insertion attempt that would have resulted in too large an overlap with any of the beads already present in the box. The boxes were then relaxed by steepest descent and conjugate gradient energy minimization, followed by equilibration runs of typically 10^8 MD steps. For the moderately entangled stars, this run time amounts to about a dozen arm end-to-end vector relaxation times and allows the polymers to diffuse over several R_g, thereby producing well equilibrated simulation boxes. Production runs to collect data for analysis lasted about 10^8 MD steps each. In some simulations the polymer centers of mass (COM) were subsequently frozen, by using rigid body translations to move their COMs back to their original positions after every integration step.

VI. RESULTS

In order to appreciate the character of the forces on centers of mass in a star polymer melt, we present in Fig. 1 a time sequence of the force in x-direction on the center of mass of

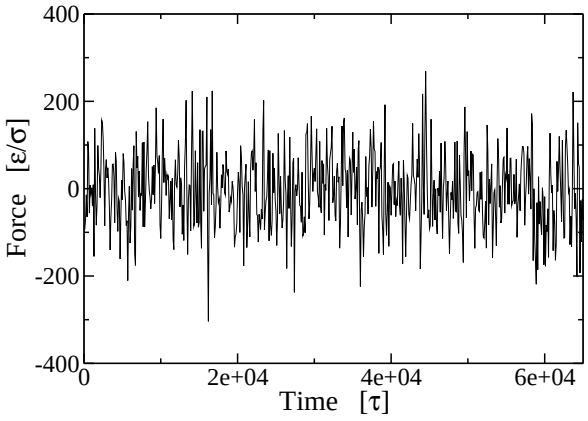

FIG. 1. Time sequence of forces in x-direction on one particular star polymer in a melt with all centers of mass fixed.

a particular star polymer in a melt in which the centers of mass of all stars were fixed. The initial configuration was taken from an equilibrium simulation with all degrees of freedom, including those of the centers of mass, free to move. It is seen that the instantaneous force fluctuates between -200 and $+200\ \epsilon/\sigma$. The average is equal to $1.75\ \epsilon/\sigma$. Obviously it will be very difficult to extract the average forces from our simulations. This can be appreciated even better from a glance of Fig. 2. In this figure we have plotted the average forces in x, y, and z-directions for all 300 stars in the box with frozen center of mass, calculated from the first 7.5×10^7 time steps after equilibration, along the horizontal axis, and those from the next 7.5×10^7 time steps along the vertical axis. Equilibration lasted 3×10^7 time steps. Averaging was done by picking frames every hundredth time step and calculating the mean. In the ideal case Fig. 2 would have been a straight line along the diagonal with positive slope. It is clear that the data still scatter substantially. Notice that for the final averages, based on 1.5×10^8 time steps, the scattering is less by a factor of $\sqrt{2}$.

Before discussing the average forces, let us take a look at Fig. 3, in which $n_0(r)$ is plotted against the distance between two stars. The inset shows the results for five different values of Δ in Eq. (29). Obviously, $n_0(r)$ increases with increasing values of Δ. In the main part of the plot, $n_0(r)/n_0(0)$ is plotted for all five values of Δ. Clearly all results are nearly equal, indicating that our normalized definition of the contact numbers n_{ij} is rather insensitive to the precise value of Δ. Also shown in this figure is the analytic representation that we fitted

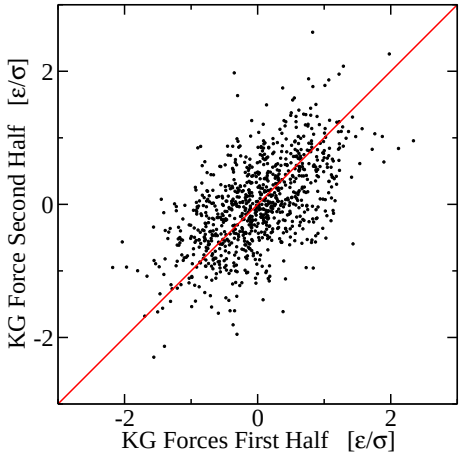

FIG. 2. All 900 Kremer-Grest(KG) forces on the centers of mass of 300 star polymers in a melt with fixed centers of mass. Values along the vertical axis are averaged over 7.5×10^7, while those along the horizontal axis are averaged over the preceding 7.5×10^7 time steps.

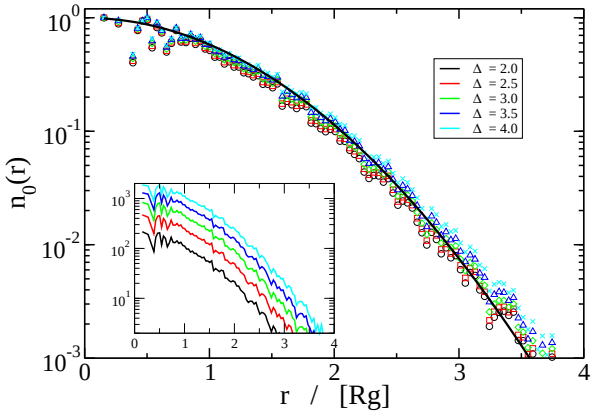

FIG. 3. Average numbers of contacts $n_0(r)$ as a function of the distance between two stars for several values of Δ in Eq. (29). The black line is a fit to the data.

to the experimental data:

$$n_0(r) = \exp\{-(\frac{r/R_g}{1.357})^2\}. \tag{39}$$

The Gaussian form was taken from Akkermans and Briels[30]. From the plot it seems safe to use a cutoff value $R_c = 3R_g$,with $R_g = 4.33\sigma$. This is somewhat larger than the $2.5R_g$ used in previous applications of the RaPiD model.

We now consider the description of the average forces by means of the extended Flory-

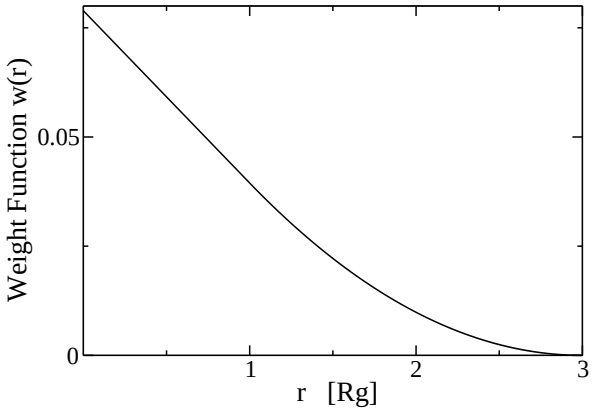

FIG. 4. Weight function $w(r)$ used to calculate local volume fraction (Eq. (18)).

Huggins model Eq. (19). In a first step we ignore the repulsive contributions, which leaves us with the pure Flory-Huggins free energy $\Phi_{\rm FH}$ and its adjustable parameters, p, χ, ρ_{max}, R_s and R_c. On the basis of their physical meanings, $n_0(r)$ and $w(r)$ must have very similar cutoff radii. In order to restrict the number of adjustable parameters we therefore choose $R_c = 3R_g$ also for the weight function. Finally we choose $R_s = 1R_g$ in order to have a smooth weight function as shown in Fig. 4.

We are now left with three adjustable parameters. Since there are no attractive forces in our small-scale simulation and the repulsions are very steep, almost all of $\Phi_{\rm FH}$ must come from entropy, which means that χ must be zero or slightly negative. Moreover, writing $\rho_{max} = r\bar{\rho}$, with $\bar{\rho}$ the overall number density, r must take values between 1.5 and 2. This follows from the fact that the volume fraction in the Kremer-Grest system is smaller than that of close packing by a factor of 1.7. Finally, also p can be roughly estimated according to $p = 3p_{arm} - 2$,with

$$p_{arm} = \frac{\langle R_{arm}^2 \rangle}{b^2} = \frac{\langle R_{arm}^2 \rangle}{C_\infty^2 l^2}, \tag{40}$$

where R_{arm} is the branch-end distance of one arm. From our simulations we found $\sqrt{\langle R_{arm}^2 \rangle} = 6.8\sigma$. Using the values $l = 0.97\sigma$ and $C_\infty = 1.80$ from the paper of Kremer and Grest[8] we get $p \simeq 43$. A somewhat smaller value of $p \simeq 40$ is obtained when the star is treated as a linear chain.

In order to determine ρ_{max}, χ and p we have performed a sequence of optimizations. We

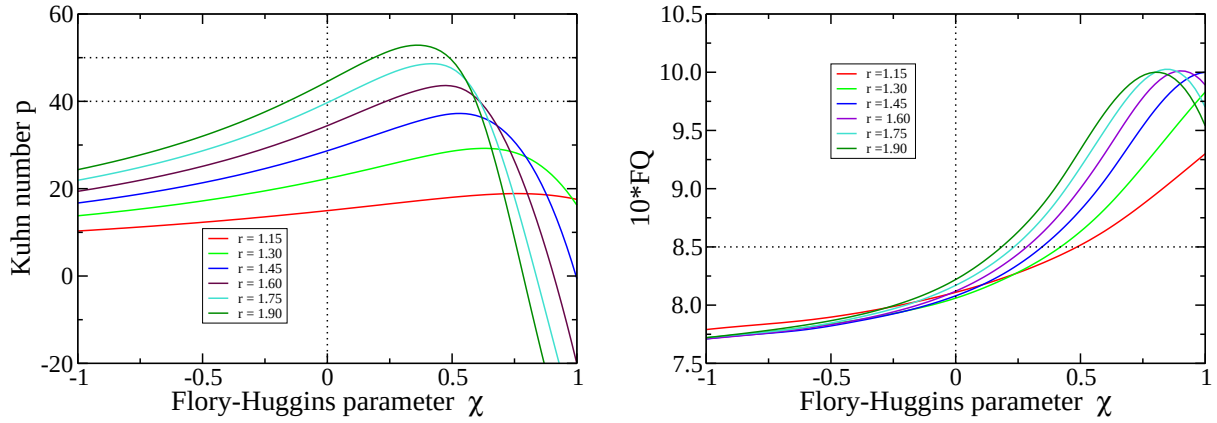

FIG. 5. Left panel: optimal number of Kuhn lengths as a function of χ for various values of $r = \rho_{max}/\bar{\rho}$. Right panel: qualities of fit FQ (multiplied by 10) corresponding to the curves in the left panel.

fixed ρ_{max} to some particular value and for a sequence of values for χ we minimized

$$D^2 = \sum_{i=1}^{2700} (F^i_{\rm FH} - F^i_G)^2 \tag{41}$$

by adjusting p. Here $F^i_{\rm FH}$ is the i^{th} force obtained with the Flory-Huggins model and F^i_G the i^{th} force obtained with the Kremer-Grest model. The resulting values of p as a function of χ are shown in Fig. 5 for several values of ρ_{max}. The corresponding qualities of fit $FQ = D_{min}/\sqrt{\langle F^2_G \rangle}$, with D^2_{min} being the minimum of D^2 and $\langle F^2_G \rangle$ the average of all 2700 forces squared obtained from the small-scale simulations with frozen centers of mass (three boxes with 300 particles each), are shown in Fig. 5. Clearly, with all values of ρ_{max}, the quality of fit becomes bad for positive Flory-Huggins parameters χ. Moreover, if one wants the number of Kuhn lengths p to be around 40, unrealistically large values of ρ_{max} are needed with decreasing values of χ. The only physically reasonable choice of parameters, still with a favourable value of FQ, seems to be $\rho_{max} = 1.9\bar{\rho}$, $\chi = 0$ and $p = 43$, in close agreement with the initial values, only the value of ρ_{max} being somewhat large.

With $\Phi_{\rm FH}(R)$ now defined, we turn our attention to $\phi^{rep}(R_{ij})$ in Eq. (19). Assuming a Gaussian function with two parameters

$$\phi^{rep}(R_{ij}) = A \exp\{-(R_{ij}/B)^2\}. \tag{42}$$

and replacing the Flory-Huggins forces in Eq. (41) by those obtained with the extended

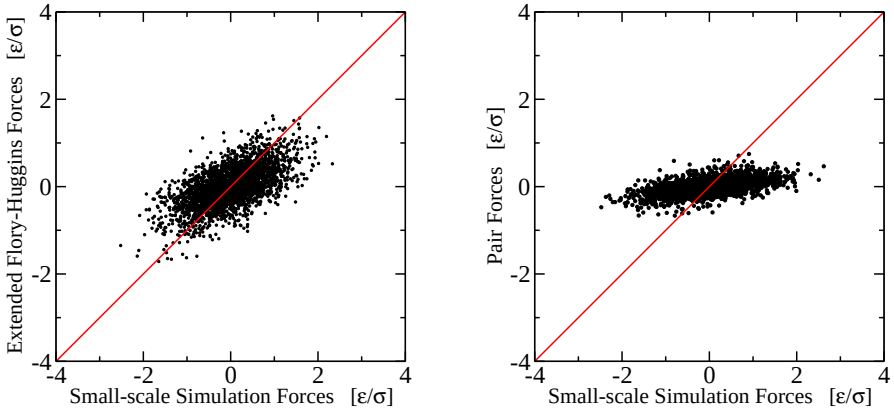

FIG. 6. Left panel: all 2700 forces on the center of mass of 900 star polymers in 3 boxes of 300 star polymers each, calculated with the extended Flory-Huggins model, along the vertical axis, and averaged over a small-scale simulation with fixed centers of mass of 1.5×10^8 time steps along the horizontal axis. Right panel: same as in left panel with extended Flory-Huggins forces replaced by pair forces from reference[33].

Flory-Huggins model, we again minimized D^2, with fixed Flory-Huggins parameters, and found $A = 1.194 k_B T$ and $B = 1.283 R_g$ with a quality of fit $FQ = 0.78$. To appreciate this result, we have plotted in Fig. 6 left panel the model forces $F^i_{\rm model}$ against the Kremer-Grest forces $F^i_{\rm G}$. For comparison we show in Fig. 6 right panel the same plot, with the model forces calculated using the pair potential of Löwen, Likos and co-workers. Clearly the extended Flory-Huggins model represents the actual average forces much better than the pair model. In Fig. 7 we show the radial distribution functions obtained with the various models. As is clear from the figure, the extended Flory-Huggins model describes the small-scale simulation very well, while the pair potential model is only marginally successful.

It should be noticed that the pair potential used for comparison in principle applies to stars in good solvent. Moreover we allowed some slight tuning of the parameters in the Flory-Huggins model, while the pair potential was applied as given in the original paper[33]. We therefore performed additional calculations (not shown) in which all parameters of the pair potential were allowed to vary in order to obtain the best agreement between simulated and model forces. It turned out that a quality of fit could be realized comparable to that obtained with the Flory-Huggins model. The corresponding parameters, however, were not physical and gave rise to completely jammed systems.

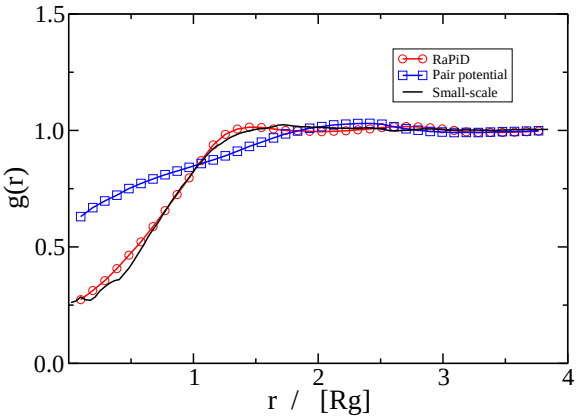

FIG. 7. Radial distribution function for centers of mass, obtained from small-scale simulation (black line), from RaPiD simulation (red line circles) and from a simulation (blue line square) with the pair potential from reference[33].

We now turn to the transient forces. As we mentioned in the previous section, we will use the equipartition theorem Eq. (31) to calculate $\alpha(R_{ij})$ from the small-scale simulation. In deriving Eq. (31) from the probability distribution Eq. (22), it was assumed that n_{ij} can take negative values, as they can do in the coarse model. With the definition given in Eq. (29), n_{ij} can only take positive values. For small values of R_{ij} this is actually not a restriction, because indeed the n_{ij} are Gaussian distributed around their mean values $n_0(R_{ij})$. With increasing values of R_{ij}, the distribution of n_{ij} begins to resemble a Poisson distribution, with the result that $\alpha(R_{ij})$ cannot be calculated from the equipartition theorem anymore. In Fig. 8 left panel we have plotted n_0 together with $n_0 + \sqrt{k_BT/\alpha}$ and $n_0 - \sqrt{k_BT/\alpha}$ as a function of r. At a distance somewhat larger than R_g, $n_0 - \sqrt{k_BT/\alpha}$ drops below zero. This is a clear indication that the Gaussian assumption does not apply anymore to the distribution of contact numbers. At the same time, the statistics is rather bad for small distances since only very few pairs exist at these distances. We therefore decided to take for α its value at $r = R_g$. In Fig. 8 right panel we have plotted the radial contact number density $4\pi r^2 \bar{\rho} g(r) n_0(r)$ as a function of the distance to a star in the origin. Clearly most contacts exist with the stars at distances between one and two R_g. This corroborates our choice to use $\alpha = \alpha(R_g)$. The values of $\alpha(r)$ are shown in Fig. 9, together with a fit $\alpha(r) \simeq 1.94 + 2.168(r/R_g)^{2.12}$, from which we obtain $\alpha(R_g) = 4.0$.

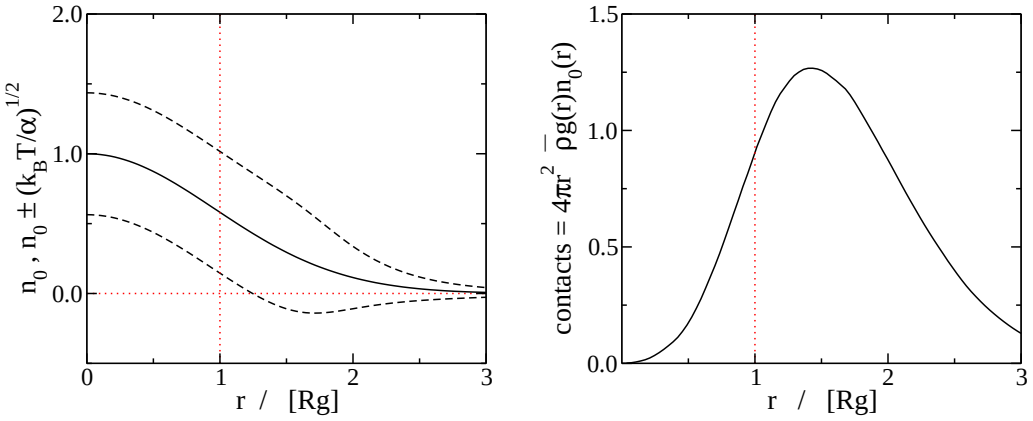

FIG. 8. Left panel: average contact number $n_0(r)$ as a function of r (black line) and $n_0(r) \pm \sigma_n$ with $\sigma_n = \sqrt{k_B T/\alpha}$ (dotted lines). Right panel: total number of contacts $4\pi r^2 \bar{\rho} g(r) n_0(r)$ as a function of r.

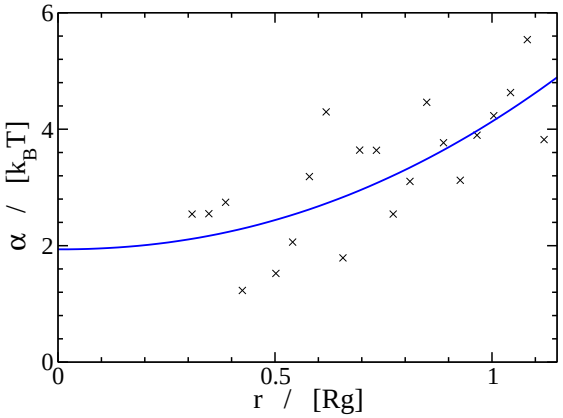

FIG. 9. Strength of transient forces α as a function of r.

The final two parameters to be calculated are ξ_0 and μ. As already mentioned in the previous section, we will use Eq. (33) to calculate μ. The left hand of this equation will be called $C(t)$. Before extracting μ, we must decide about the time scale on which we should calculate $C(t)$. According to our general picture of the dynamics of the stars, the arms relax towards equilibrium dictated by the collection $\{n_0(R_{ij})\}$. These numbers will have changed, however, as soon as all stars have diffused appreciably, let's say over distances of about $0.1 \sim 0.2 R_g$. From our small-scale simulations we found that such displacements correspond to about 310τ. In Fig. 10 we have plotted $C(t)$ for times up to 650τ. We observe two

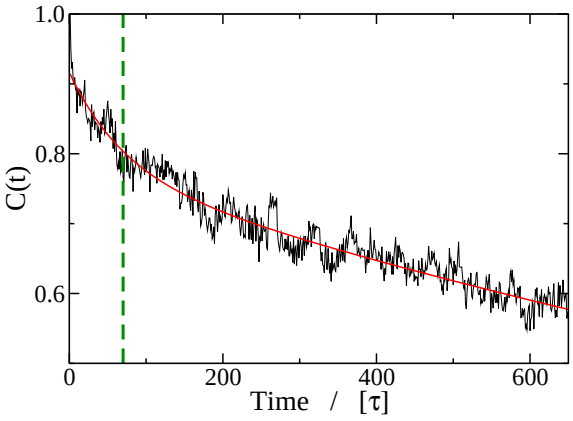

FIG. 10. Decay curves $C(t)$ (left hand side of Eq. (33)) as a function of time lapse since freezing the centers of mass motion. The dashed line indicates the time when in the free box the centers of mass have moved over 0.15 R_g.

exponential decays, the first of which corresponds to our μ. From a fit with two exponents we obtain $C(t) = 0.7762 \times e^{(-t/75)} + 0.14 \times e^{(-t/219)}$ and so $\mu = 75\tau$.

The friction per contact, ξ_0, is extremely difficult to measure from small scale simulations. We therefore choose to follow a pragmatic route by adjusting ξ_0 until the progressive diffusion coefficient

$$D(t) = \frac{1}{6t}\langle(\vec{R}_i(t) - \vec{R}_i(0))^2\rangle. \tag{43}$$

is well represented by the coarse model. In Fig. 11, $D(t)$ is plotted as a function of time, once using the RaPiD model and once using the Kremer-Grest model. With $\xi_0 = 265m/\tau$ the final diffusion coefficient $D = \lim_{t\to\infty} D(t)$ is well represented by the RaPiD model. Of course at the very early times RaPiD cannot reproduce the correct dynamics because it is driven by a sequence of processes at time scales that have been replaced by a Markovian friction plus corresponding noise. Also at the intermediate times RaPiD is not very successful.

At this point, all parameters of the RaPiD model have been calculated from an underlying small scale simulation. If the model captures the real physics it should now reproduce all physical properties without any additional parameter tuning. Therefore we calculated the shear relaxation modulus

$$G(t) = \frac{V}{k_B T}\langle\sigma_{xy}(t)\sigma_{xy}(0)\rangle, \tag{44}$$

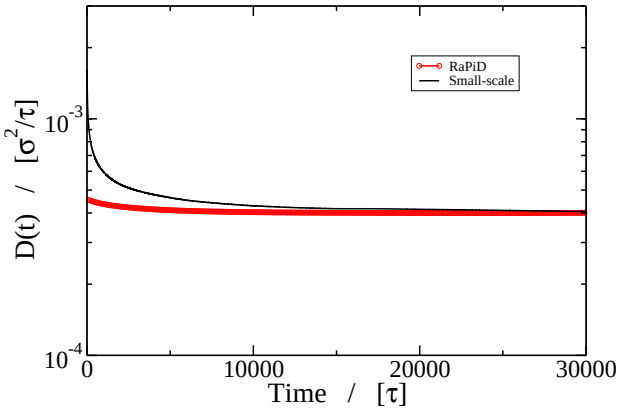

FIG. 11. Progressive diffusion coefficient as a function of time from small-scale simulation (black line) and from RaPiD run (symbols).

with σ_{xy} being the xy element of the stress tensor calculated according to

$$\sigma_{xy} = -\frac{1}{V}\sum_{ij}(R_{i,x} - R_{j,x})F_{ij,y}. \tag{45}$$

In the last equation, $R_{i,x}$ is the x-coordinate of the position vector of particle i and $F_{ij,y}$ is the y-component of the force exerted by particle j on particle i. The results are shown in Fig. 12. Clearly, the results obtained with the small-scale simulation are very noisy. This is a well known fact with all small scale simulations, which is due to the fact that the stress-stress auto-correlation function in Eq. (46) is calculated from just one single, heavily fluctuating quantity, as opposed to auto-correlation functions of single particle properties, which fluctuate less wildly and moreover may be averaged over all particles in the box. The shear relaxation modulus obtained with the coarse model ignoring the transient forces, by always putting $n_{ij} = n_0(R_{ij})$, reproduces the small-scale simulation data at long times surprisingly well. At intermediate times, clearly the transient forces are needed to reproduce the $G(t)$ of small-scale simulation. The full RaPiD curve roughly exhibits two relaxations. This should not be surprising since with $\sigma_{xy} = \sigma^{th}_{xy} + \Delta\sigma_{xy}$ and $\langle\Delta\sigma_{xy}(t)\sigma^{th}_{xy}(0)\rangle = \langle\Delta\sigma_{xy}(0)\sigma^{th}_{xy}(t)\rangle = 0$ we obtain

$$G(t) = \frac{V}{k_BT}\{\langle\sigma^{th}_{xy}(t)\sigma^{th}_{xy}(0)\rangle + \langle\Delta\sigma_{xy}(t)\Delta\sigma_{xy}(0)\rangle\}. \tag{46}$$

Here σ^{th}_{xy} is the xy-stress contribution from the thermodynamic forces and $\Delta\sigma_{xy}$ the remaining part, contributed by the transient forces. The vanishing of the cross correlations $\langle\Delta\sigma_{xy}(t)\sigma^{th}_{xy}(0)\rangle$ is due to the fact that with every configuration of the center of mass the

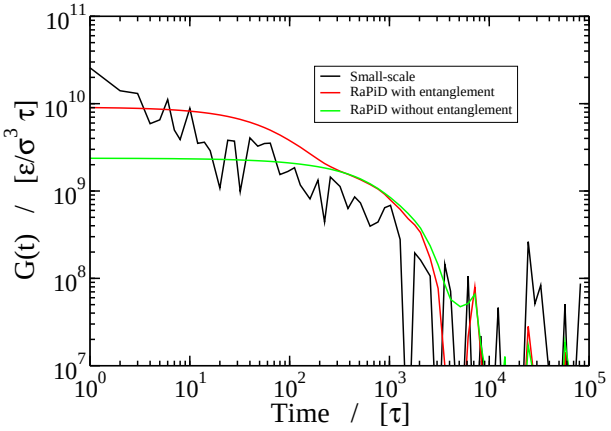

FIG. 12. Shear relaxation modulus from small-scale simulation (black line) and from RaPiD run (red line); the green line represents the contribution from the conservative forces.

transient forces fluctuate around zero. Even when the order of magnitude and the covered time regimes are correct it is clear that the model is too simple to capture all the details of the shear relaxation modulus at intermediate times. In previous applications of the RaPiD model, we have shown that with some simple adjustments, like in Eq. (27) or allowing for deformation of the coarse particle[28], very good results may be obtained. Here we have shown that the successes of the RaPiD model are not just sheer luck, but that all parameters indeed have a well defined physical meaning. Our limitations in this paper have basically been due to difficulties to run sufficiently long small scale simulations.

VII. SUMMARY AND CONCLUSIONS

We have presented a method to calculate all functions and parameters in the responsive particle model (RaPiD) from an underlying small scale simulation. RaPiD is a coarse grain model in which every polymer is represented by a single point particle dressed with additional variables to describe the dominant effects of the eliminated degrees of freedom. In order to conserve both the thermodynamic and the dynamic properties of the original model, forces are considered to consist of two contributions. The first contribution is taken to be the average forces for given, instantaneous positions of the particles. The remaining contribution is modelled by an additional set of dynamical variables for each pair within a certain cutoff distance.

The average forces are taken to derive from a potential with implicit many-body contributions based on the Flory-Huggins model, to properly take care of the entropy of the eliminated degrees of freedom. With a previously suggested definition of local volume fractions all parameters in the model may be estimated on the basis of their physical meaning. With only very small tuning of these parameters around the estimated values very good agreement between actual and model forces was obtained. Moreover, the radial distribution function obtained with the model was in excellent agreement with the one obtained with the small scale simulation. Similar agreement could not be obtained with the best effective pair potential model available, not even by optimising all parameters in the model to achieve good agreement with the actual forces, since this led to unphysical results. We conclude that many-body terms are an important ingredient in coarse grain models for polymer melts and dense solutions. This is in agreement with conclusions drawn before by the authors of the pair model discussed in the paper[46] and in a paper by Hijón *et al.*[47], even when they dealt with stars of high functionality and small arms.

It is interesting to notice that the cut-off radius of the weight function $w(r)$ needed to calculate correct forces must be larger than we have used in previous papers. Calculations with smaller cut-off radii (not shown) turned out to lead to unphysical parameters, while still not leading to the qualities of fit presented in the previous section. The necessity to include long-range interaction is reminiscent of the long-range attractive tail in the work of Guenza *et al.*[48]. It is difficult, however to analyze the implicitly many-body potential used in the present paper in terms of effective two-body potentials. We leave this for future investigation.

The fluctuating forces are larger than the average forces by two orders of magnitude. This fact alone is enough to conclude that it will be impossible to describe both the thermodynamic properties and the dynamic properties correctly on the basis of a simple conservative forcefield involving only the positions of the polymers. In the RaPiD model the fluctuating forces are described by so called contact numbers, whose dynamics brings into the simulation the memory effects resulting from the elimination of the internal degrees of freedom of the polymers. We have measured the root mean square deviations from their equilibrium values and the corresponding decay times of these contact numbers. This left us with one parameter that we adjusted to have the diffusion coefficient correct. The shear relaxation modulus as a function of time was next found to be correctly reproduced by the coarse

model, albeit not in all its details.

It is perhaps useful to stress that in this paper, we use a first order propagator to advance the system in time. The reason for this is that we are interested in highly damped system, i.e. system with large frictions. The first order propagator allows the use of increasingly large time steps with increasing frictions, while the opposite holds true for second order propagator. An early example of the use of a second order propagator is to be found in the work of Akkermans and Briels[38, 49], where the Mori-Zwanzig projector operator formalism to obtain the propagator is described in detail. The formalism gives rise to time dependent frictions, describing the coupling between the coarse degrees of freedom and the eliminated small scale degrees of freedom. Expressions for the friction kernels involve the 'projected dynamics' of the small scale system, which is difficult to extract from the actual dynamics. Usually one assumes that the projected dynamics may simply be replaced by the real dynamics[38]. Recently Vanden-Eijnden and coworkers developed a method to bypass these problems[47, 50], obtaining results for melts of star polymers with relatively short arms. In the present paper we bypass the problem by extending the set of 'relevant variables' until they may be assumed to be Markovian. It is then a simple step to convert the second order propagator to a first order propagator[39] and take advantage of its properties.

In summary we conclude that splitting forces into average forces and transient forces is a very promising concept. Average forces require many-body contributions, which can be modelled very well. The present implementation of the transient forces performs rather well. Our calculations have revealed, however, that there is still quite some room for amelioration of the modelling of the transient forces. We mention three possible ways to attack this problem. First, it is conceivable that, depending on the application, better definitions exist for the variables n_{ij}. Second, other distributions than the Gaussian distribution for the n_{ij} should be considered. Finally, ways to implement a range of characteristic times into the dynamics of the n_{ij} should be developed. This latter point seems to be the most fundamental of all, as can be clearly seen by glancing at Fig. 11 and Fig. 12. While the shear relaxation modulus is described rather well on all time scales - recall that no fine tuning was performed to achieve the best results - the diffusion coefficient is not well described at shorter times. This would, for example, be immediately seen in neutron spin echo experiments. Apparently the eliminated dynamics occurs at a range of time scales, with each time scale having different effects on $G(t)$ and $D(t)$ respectively.

The most reliable way to solve these problems is to possibly extend the number of additional variables, and to derive their dynamics from theories addressing the details of the small scale dynamics[1–3, 9]. This will also reveal the dependence of our model parameters on architectural parameters of the molecules. For the time being the present work provides a proof of principle.

ACKNOWLEDGMENTS

The authors acknowledge financial support from the European Union's Seventh Framework Programme (FP7) through the Marie Curie initial training network DYNamics of Architecturally Complex Polymers (DYNACOP), grant agreement 214627, and the European Soft Matter Infrastructure (ESMI), grant agreement 262348.

[1] M. Doi and S. F. Edwards, *The Theory of Polymers Dynamics* (Oxford Science Publications, Oxford, U. K., 1986).

[2] P. G. de Gennes, *Scaling Concepts in Polymer Physics* (Cornell University Press, Ithaca, New York, 1979).

[3] T. C. B. McLeish, Advances in Physics **51**, 1379 (2002).

[4] J. T. Padding and W. J. Briels, J. Phys. Condens. Matter **23**, 233101 (2011).

[5] Y. Li, B. C. Abberton, and M. Kröger, Polymers **5**, 751 (2013).

[6] S. D. Anogiannakis, C. Tzoumanekas, and D. N. Theodorou, Macomolecules **45**, 9475 (2012).

[7] V. A. Harmandaris and K. Kremer, Macromolecules **42**, 791 (2009).

[8] K. Kremer and G. S. Grest, J. Chem. Phys **92**, 5057 (1990).

[9] M. Guenza, J. of Phys.: Condensed Matter **20**, 033101 (2008).

[10] P. Kindt and W. Briels, J. Chem. Phys. **127**, 134901 (2007).

[11] J. T. Padding and W. J. Briels, J. Chem. Phys. **115**, 2846 (2001).

[12] J. T. Padding and W. J. Briels, J. Chem. Phys. **117**, 925 (2002).

[13] L. Liu, J. T. Padding, W. K. den Otter, and W. J. Briels, J. Chem. Phys. **138**, 244912 (2013).

[14] Y. Masubuchi, J. I. Takimoto, K. Koyama, G. Ianniruberto, G. Marrucci, and F. Greco, J. Chem. Phycs. **115**, 4387 (2001).

[15] R. G. Larson, *The Structure and Rheology of Complex Fluids* (Oxford University Press, Oxford, U. K., 1999).

[16] R. B. Bird, R. C. Armstrong, and O. Hassager, *Dynamics of Polymeric Liquids, Volume 1, Fluid Mechanics, 2nd Edition* (John Wiley & Sons, Inc., United states of America, 1987).

[17] V. Schmitt, C. M. Marques, and F. Lequeux, Phys. Rev. E **52**, 4009 (1995).

[18] J. K. G. Dhont, K. Kang, M. P. Lettinga, and W. J. Briels, Korea-Australia Rheology Journal **22**, 291 (2010).

[19] A. van den Noort, W. K. den Otter, and W. J. Briels, Europhys. Lett. **80**, 28003 (2007).

[20] W. J. Briels, Soft Matter **5**, 4401 (2009).

[21] A. van den Noort and W. Briels, J. Non-Newt. Fluid Mech. **152**, 148 (2008).

[22] A. van den Noort and W. Briels, Macromol. Theory Simul. **16**, 742 (2007).

[23] I. S. de Oliveira, A. van den Noort, J. T. Padding, W. K. den Otter, and W. J. Briels, J. Chem. Phys. **135**, 104902 (2011).

[24] I. S. de Oliveira, W. K. den Otter, and W. J. Briels, EuroPhys. Lett. **101**, 28002 (2013).

[25] J. T. Padding, L. V. Mohite, D. Auhl, W. J. Briels, and C. Bailly, Soft Matter **7**, 5036 (2011).

[26] J. Padding, L. Mohite, D. Auhl, T. Schweizer, W. Briels, and C. Bailly, Soft Matter **8**, 7967 (2012).

[27] G. J. Schneider, K. Nusser, S. Neueder, M. Brodeck, L. Willner, B. Farago, O. Holderer, W. J. Briels, and D. Richter, Soft Matter **9**, 4336 (2013).

[28] I. S. de Oliveira, B. Fitzgerald, W. K. den Otter, and W. J. Briels, J. Chem. Phys. **140**, 104903 (2014).

[29] S. Singh, R. G. Winkler, and G. Gompper, Phys. Rev. Lett. **107**, 158301 (2011).

[30] R. L. C. Akkermans and W. J. Briels, J. Chem. Phys. **114**, 1020 (2001).

[31] C. N. Likos, Physics Reports **348**, 267 (2001).

[32] C. N. Likos, H. Löwen, M. Watzlawek, B. Abbas, O. Jucknischke, J. Allgaier, and D. Richter, Physical Review Letters **80**, 4450 (1998).

[33] A. Jusuf, J. Dzubiella, C. N. Likos, C. von Ferber, and H. Löwen, Journal of Physics: Condensed Matter **13**, 6177 (2001).

[34] F. Schmid, J. Physics-Condensed Matter **10**, 8105 (1998).

[35] I. Pagonabarraga and D. Frenkel, J. Chem. Phys. **115**, 5015 (2001).

[36] S. Y. Trofimov, E. L. F. Nies, and M. A. J. Michels, J. Chem. Phys. **117**, 9383 (2002).

[37] J. M. Deutch and I. Oppenheim, J. Chem. Phys. **54**, 3547 (1971).

[38] R. L. C. Akkermans and W. J. Briels, J. Chem. Phys. **113**, 6409 (2000).

[39] D. L. Ermak and J. A. McCammon, J. Chem. Phys. **69**, 1352 (1978).

[40] S. Kjelstrup, D. Bedeaux, E. Johannessen, and J. Gross, *Non-Equilibrium Thermodynamics for Engineers* (World Scientific, 2010).

[41] J. Sprakel, E. Spruijt, J. van der Gucht, J. T. Padding, and W. J. Briels, Soft Matter **5**, 4748 (2009).

[42] W. J. Briels and H. L. Tepper, Physical Review Letters **79**, 5074 (1997).

[43] D. Chandler, *Introduction to Modern Statistical Mechanics* (Oxford University Press, USA, 1987).

[44] B. Hess and C. Kutzner and D. van der Spoel and E. Lindahl, J. Chem. Theory Comput. **4**, 435 (2008).

[45] G. S. Grest and K. Kremer, Phys. Rev. A **33**, 3628 (1986).

[46] C. von Ferber, A. Jusufi, C. Likos, H. Löwen, and M. Watzlawek, The Euro. Phys. J. E **2**, 311 (2000).

[47] C. Hijón, P. Español, E. Vanden-Eijnden, and R. Delgado-Buscalioni, Faraday Discuss. **144**, 301 (2010).

[48] J. McCarty, A. J. Clark, I. Y. Lyubimov, and M. G. Guenza, Macromolecules **45**, 8482 (2012).

[49] J. Padding and W. Briels, Nanostructured soft matter, A.V. Zvelindovsky edition, Springer (2007).

[50] A. Majda, I. Timofeyev, and E. Vanden-Eijnden, Nonlinearity **19**, 769 (2006).

Shear relaxation modulus for star polymers (3 arms, 35 beads each) reproduced by single particle model including transient force.